Available online at www.sciencedirect.com
SCIENCE DIRECT®
Journal of Solid State Chemistry 178 (2005) 2818–2824
JOURNAL OF SOLID STATE CHEMISTRY
www.elsevier.com/locate/jssc

Constitution of the Sr–Ni–O system

M. Zinkevich*

Max-Planck-Institut für Metallforschung and Institut für Nichtmetallische Anorganische Materialien der Universität Stuttgart, Heisenbergstraße 3, D-70569 Stuttgart, Germany

Received 5 April 2005; received in revised form 8 June 2005; accepted 21 June 2005

Abstract

The constitution of the Sr–Ni–O system was studied experimentally for the first time. Samples were prepared either from $SrCO_3$ and NiO or from $Sr(NO_3)_2$ and $Ni(NO_3)_2 \cdot 6H_2O$ and characterized by high-temperature X-ray powder diffraction, scanning electron microscopy, thermogravimetric and differential thermal analyses. In the SrO–NiO quasibinary system an eutectic reaction: liquid $\rightleftharpoons$ SrO + NiO was found to occur at $1396 \pm 5\,^{\circ}C$, while the homogeneity range of terminal solid solutions is negligible. Thermodynamic calculations using the regular solution model for the liquid and rocksalt-type phases were employed to predict liquidus and solidus curves. Three ternary compounds, $SrNiO_{2.5}$, $Sr_5Ni_4O_{11}$, and $Sr_9Ni_7O_{21}$ were observed in the samples prepared from nitrate solutions, but only $Sr_9Ni_7O_{21}$ was proved to be thermodynamically stable in air up to $1030 \pm 6\,^{\circ}C$. When heating in air, $SrNiO_{2.5}$ and $Sr_5Ni_4O_{11}$ were found to transform irreversibly into a mixture of $Sr_9Ni_7O_{21}$ and NiO. Isothermal section of the SrO–NiO–O subsystem, which represents phase equilibria at 950–1030 °C as well as an isobaric section of the Sr–Ni–O system in air were constructed.

Keywords: Strontium; Nickel; Oxygen; Phase diagram; Ternary compounds; Thermal stability

1. Introduction

Nickel oxide is known to form a variety of perovskite-related phases with oxides of strontium and barium depending on the oxidation state of Ni-ions [1]. The simplest compounds containing Ni^{2+}, Ni^{3+}, and Ni^{4+} have formulas $MNiO_2$, $MNiO_{2.5}$, and $MNiO_3$ (M = Sr, Ba), respectively [2]. In addition, mixed-valence compounds, e.g., $Sr_4Ni_3O_9$ [3], $Sr_9Ni_7O_{21}$ [4], $Sr_{12}Ni_{7.5}O_{27}$ [1], $Ba_{18}Ni_{15}O_{45}$ [5] have been reported to exist. Most of them are ordered structures, which are built up by the stacking of layers derived from perovskite structure [6]. The relative stability of various compounds in a system is known from the equilibrium phase diagram. Among the alkaline-earth elements, phase relations in the M–Ni–O systems are established for M = Mg, Ca and Ba. The comparison of those phase diagrams reveals a regularity, which is determined by ionic radii of M^{2+} ions [7]. At ambient pressure, all the monoxides MO and NiO crystallize in the rocksalt-type structure. The effective ionic radius of Mg^{2+} in six-fold coordination (72 pm) is very close to that of Ni^{2+} (70 pm) and a quasibinary phase diagram MgO–NiO shows the formation of continuous solid and liquid solutions [8]. The effective ionic radii of Ca^{2+} and Ba^{2+} are 100 and 136 pm, respectively, and a significant size mismatch is reflected in the phase diagrams. The quasibinary system CaO–NiO is of simple eutectic type with a miscibility gap in the solid state [9], while the intersolubility of BaO and NiO is very small, but compounds $BaNiO_2$ and Ba_3NiO_4 are formed [10]. Quantitatively, this can be expressed in terms of free energy of mixing or free energy of formation for a solid solution or a compound, respectively. The Sr–Ni–O system is a missing chain in the above analysis, since the phase diagram has not been investigated so far, although there is an evidence for the

*Fax: +49 711 68 93 131.
E-mail address: zinkevich@mf.mpg.de.
URL: http://aldix.mpi-stuttgart.mpg.de/zinkevit/home_mz.html.

0022-4596/$ - see front matter © 2005 Elsevier Inc. All rights reserved.
doi:10.1016/j.jssc.2005.06.035

existence of intermediate phases. From the effective ionic radius of Sr^{2+} (116 pm), both the solid solubility and compound formation can be expected. Theoretical calculations, which made use of interionic potentials for dilute solid solutions to evaluate the excess free energy showed that mutual solid solubility in SrO–NiO subsystem can be as high as 25 mol% [11].

In the present work, experimental study of phase equilibria in the Sr–Ni–O system was complemented by thermodynamic calculations.

2. Assessment of the literature information

The assessed literature information on the ternary phases of the Sr–Ni–O system is compiled in Table 1. $SrNiO_2$ crystallizes in the orthorhombic cell with square planar coordinated Ni^{2+} ions and is isotypic with $SrCuO_2$—the derivative of the K_2NiF_4-type structure [12]. Single crystals of $SrNiO_2$ have been grown from the melt of equimolar mixture of SrO and NiO at 150 bar O_2 [12]. Harwood and co-workers [16] attempted to prepare $SrNiO_2$ by heating $SrCO_3$ and NiO in vacuum at 960 °C, but no reaction between the resulting SrO and NiO has been observed. Subsequently, a synthesis of $SrNiO_2$ by solid-state reaction has been reported [2], but the sample contained significant amount of unreacted NiO.

Compound with formula $SrNiO_{2.5}$ (or $Sr_2Ni_2O_5$) has been reported to form above 600 °C under a wet oxygen atmosphere [13]. Arjomand and Machin synthesized $SrNiO_{2.5}$ by heating $Sr(NO_3)_2$ and $Ni(NO_3)_2$ in air at 670 °C [2]. The crystal structure of $SrNiO_{2.5}$ has not been determined, however X-ray patterns were indexed assuming hexagonal unit cell [2,13]. The lattice parameters of $SrNiO_{2.5}$ vary with the preparation conditions.

$SrNiO_3$, which contains tetravalent nickel, has been obtained at 600 °C under a high pressure of oxygen between 50 and 2000 bar [2,13]. It adopts a perovskite-like structure of $BaNiO_3$-type with two-layer hexagonal close packing. At ambient oxygen pressure, $SrNiO_3$ becomes oxygen-deficient and transforms into $SrNiO_{2.5}$ above 600 °C [2,13].

Compounds $Sr_4Ni_3O_9$ (or $Sr_5Ni_4O_{11}$) [3,14], $Sr_9Ni_7O_{21}$, which is a member of the series $Sr_{3n+3}Ni_{2n+3}O_{6n+9}$ ($n = 2$) [4,6], and $Sr_{12}Ni_{7.5}O_{27}$ [1] have been obtained as single crystals from potassium hydroxide melts, while $Sr_3Ni_{12}O_{24}$ has been prepared by cation exchange with $K_{0.23}NiO_2 \cdot nH_2O$ [15]. Their structural data are given in Table 1. Both $Sr_4Ni_3O_9$ and $Sr_5Ni_4O_{11}$ gave the same XRD powder pattern [3,14]. However, crystals of $Sr_5Ni_4O_{11}$ and $Sr_{12}Ni_{7.5}O_{27}$ were found to contain potassium in detectable amounts [1,14], so that a possible stabilization of such structures by K^+ cations cannot be ruled out.

There is a lack of information in the literature on the constitution and thermodynamics of the Sr–Ni–O system. From the experiments of Pausch and Müller-Buschbaum [12], it can be inferred that $SrNiO_2$ may show a congruent melting behavior. In addition, one may expect that phase equilibria will be significantly affected by the variation of oxygen pressure in the gas phase.

Table 1
Ternary phases in the Sr–Ni–O system (literature data)

Phase	Pearson symbol	Space group	Prototype	Lattice parameters (nm)	Reference
$SrNiO_2$	*oC*16	*Cmcm*	$SrCuO_2$	$a = 0.3581$ $b = 1.6362$ $c = 0.3915$	[12]
$SrNiO_{2.5}$	*h***	—	—	$a = 0.5465(1)$[a] $c = 0.4137(1)$[a]	[13]
$SrNiO_3$	*hP*10	$P6_3/mmc$	$BaNiO_3$	$a = 0.5355(1)$ $c = 0.4860(1)$	[13]
$Sr_{12}Ni_{7.5}O_{27}$	*hP*48	*P*321	—	$a = 0.9474(4)$ $c = 0.7802(7)$	[1]
$Sr_4Ni_3O_9$ $Sr_5Ni_4O_{11}$	*hP*57	*P*321	—	$a = 0.9477(1)$ $c = 0.7826(4)$	[3] [14]
$Sr_9Ni_7O_{21}$	*hR*270	$R\bar{3}c$	—	$a = 0.9524(2)$ $c = 3.6008(5)$	[4]
$Sr_3Ni_{12}O_{24}$	*hR*39	$R\bar{3}m$	—	$a = 0.566$ $c = 1.769$	[15]

[a]Sample prepared at 600 °C and 1 bar O_2.

3. Experimental procedures

Two series of samples for the experimental investigation were prepared using different methods. In a *first series*, $SrCO_3$ (Sigma Aldrich GmbH, Steinheim, Germany, 99.9+%) and NiO (Merck KgaA, Darmstadt, Germany, extra pure) were used as starting materials. Eleven samples with Sr:Ni atomic ratio of 10:90, 20:80, 25:75, 30:70, 40:60, 50:50, 60:40, 70:30, 75:25, 80:20, and 90:10 mol% NiO were prepared. The powders were mixed and ground in ethanol using an agate ball mill for 2 h, dried at 65 °C and calcined at 1100 °C in air for 24 h in corundum crucibles. In a *second series*, $Sr(NO_3)_2$ and $Ni(NO_3)_2 \cdot 6H_2O$ (Merck KgaA, Darmstadt, Germany, analytical grade) were dissolved in deionized water, the solution was transferred into evaporating dish and heated at 100 °C on the hot plate until the solid residual was obtained. Upon further heating up to 500 °C in air the nitrates decomposed and a black substance was produced, which was then calcined at 600 °C for 3 h. Samples with nominal Sr:Ni atomic ratio of 20:80, 48:52, 49:51, 51:49, 52:48, and 54:46 were prepared by this route. The actual chemical composition of the second series samples (Sr, Ni, and C) was determined by inductively coupled plasma optical emission spectroscopy (ICP-OES; Model CIRO, Spectro Inc.) and carrier-gas hot extraction technique (Water-Carbon-Analyzer; Model CWA 5003, Fisher-Rosemount, Hanau).

The calcined powders of both series were ground in an agate mortar, cold-isostatically pressed into pellets at 625 MPa (1 min), and sintered in air at various temperatures in corundum crucibles. After heat-treatment, the samples were either furnace cooled (initial cooling rate 10 °C min^{-1}) or quenched in air (hot specimens were quickly transferred from the tubular furnace onto the massive copper plate at room temperature).

Fired materials were characterized ex situ by X-ray powder diffraction analysis (XRD; Model D5000, Siemens AG, Karlsruhe, Germany) with position-sensitive detector, Cu$K\alpha$ radiation, $2\Theta = 10-90°$, $\Delta 2\Theta = 0.016°$, and a counting time of 1 s. Silicon powder (Sigma Aldrich GmbH, Steinheim, Germany, 99.999%) was used as internal standard. Assignment of the particular phases to the diffraction maxima was carried out using PDF database of the International Center for Diffraction Data (ICDD) [17] and Inorganic Crystal Structure Database (ICSD) [18]. In addition, three samples with Sr:Ni atomic ratio of 20:80, 48:52, and 52:48 were studied in situ by high-temperature X-ray powder diffraction analysis (HTXRD, Model D500, Siemens AG, Karlsruhe, Germany) using Cu$K\alpha$ radiation, a position sensitive detector (MBraun) and a PAAR HTK10 high temperature chamber. The powdered samples were strewn upon a platinum heating tape. All measurements were performed in the 2Θ range between 15° and 60° with $\Delta 2\Theta = 0.02°$, and a counting time of 1 s in air. Thermogravimetric and differential thermal analysis (TG/DTA; Model STA 409C, NETZSCH-Gerätebau GmbH, Selb, Germany) was carried out using alumina crucibles as a sample container and as a reference. Polished compact samples with Sr:Ni atomic ratio of 49:51 and 51:49 were analyzed by scanning electron microscopy (SEM) in the backscattered electron imaging mode with energy-dispersive X-ray analysis (EDX) using DSM 982 Gemini device operating at 20 kV and 10 nA with a standard error of ±0.5 wt% and a CoKa line calibration element.

4. Results and discussion

4.1. Reaction of strontium carbonate with nickel oxide

TG/DTA heating curves of the mixtures of $SrCO_3$ and NiO showed the typical pattern of thermal decomposition of $SrCO_3$ with onset temperature of 930 °C and an endothermic peak with an onset temperature of 1396 ± 5 °C without any weight loss. The latter was interpreted as an eutectic melting, i.e., liquid $\rightleftharpoons$ SrO + NiO. Thermal effects on cooling were not reproducible since the melt reacted with alumina crucible. To check the possible effect of Al_2O_3 on the melting temperature, the sample with Sr:Ni atomic ratio of 60:40 was heated in platinum container up to 1400 °C. The formation of the liquid phase in this sample as well as in all samples after TG/DTA was confirmed by visual observation. XRD analysis of the solidified melt showed the presence of SrO and NiO only. When the mixtures of $SrCO_3$ and NiO were annealed at 1300 or 1200 °C for 153 h, only SrO and NiO phases were found on the XRD patterns. No peaks shift with respect to the reference values for pure SrO and NiO [17] has been observed independent of composition. This indicates a negligible mutual solid solubility between SrO in NiO.

4.2. Ternary phases formed from nitrate solution and their thermal stability

Results of chemical analysis of the second series samples (prepared from nitrate solution) are given in Table 2. Samples calcined at 670 °C (SN2, SN4) contained few atomic percents of carbon, due to the presence of $SrCO_3$. The latter was observed in the corresponding XRD patterns (see below) and seems to form through the side reaction with atmospheric CO_2 during thermal decomposition of strontium nitrate. The calcination at 920 °C resulted in carbon-free samples, when the Sr:Ni atomic ratio was less than unity (SN1, SN3). Samples containing more Sr (SN5, SN6) showed

Table 2
Results of chemical analysis of the Sr–Ni–O samples prepared from nitrate solution

Sample	Sr:Ni ratio	Heat-treatment	Sr (at%)	Ni (at%)	C (at%)	O (at%)[a]
SN1	20:80	Air, 920 °C, 48 h	9.7±0.1	37.2±0.3	0	53.1
SN2	48:52	Air, 670 °C, 24 h	20.3±0.2	21.7±0.2	1.6±0.1	56.4
SN3	49:51	Air, 920 °C, 132 h	20.7±0.2	21.7±0.2	0	57.6
SN4	51:49	Air, 670 °C, 96 h	21.9±0.2	20.7±0.2	0.60±0.07	56.8
SN5	52:48	Air, 920 °C, 48 h	22.8±0.2	20.6±0.2	0.30±0.03	56.3
SN6	54:46	Air, 920 °C, 48 h	23.4±0.2	20.1±0.2	0.40±0.03	56.1

[a]Calculated from mass balance.

Table 3
Results of phase analysis of the Sr–Ni–O samples prepared from nitrate solution and furnace cooled after heat treatment as determined by XRD and SEM-EDX

Sample	Sr:Ni ratio	Heat treatment (cooling at 10 °C min^{-1})	Observed phases (PDF Card number [17])[a]
SN1	20:80	Air, 920 °C, 48 h	NiO (47-1049), $Sr_9Ni_7O_{21}$
SN2	48:52	Air, 670 °C, 24 h	$SrNiO_{2.5}$ (28-1242), NiO (47-1049), $SrCO_3$ (05-0418)
SN3	49:51	Air, 650 °C, 24 h	$SrNiO_{2.5}$ (28-1242), NiO (47-1049), $SrCO_3$ (05-0418)
SN3[b]	49:51	Air, 920 °C, 132 h	$Sr_9Ni_7O_{21}$, NiO (47-1049)
SN4	51:49	Air, 670 °C, 96 h	$SrNiO_{2.5}$ (28-1242)[c], $Sr_5Ni_4O_{11}$(42-0521)[c], NiO (47-1049), $SrCO_3$ (05-0418)
SN5[b]	52:48	Air, 920 °C, 48 h	$Sr_9Ni_7O_{21}$, NiO (47-1049), $SrCO_3$ (05-0418)
SN6[b]	54:46	Air, 920 °C, 48 h	$Sr_9Ni_7O_{21}$, NiO (47-1049), $SrCO_3$ (05-0418)

[a]Compound $Sr_9Ni_7O_{21}$ was identified according to ICSD [18].
[b]Unidentified peaks present (cf. Fig. 1).
[c]Lattice parameters are different from [17].

the traces of $SrCO_3$ even after heat treatment at 920 °C (Table 2).

Results of phase analysis of the furnace-cooled samples are summarized in Table 3. After heat treatment of the SN3, SN5, and SN6 samples at higher temperature, neither $SrNiO_{2.5}$ nor $SrCO_3$ were observed, while the main phase became $Sr_9Ni_7O_{21}$. At the same time, additional diffraction maxima have emerged (Fig. 1), which could not be associated with any known compounds in the Sr–Ni–O system. Those reflections appear as doublets (marked with stars in Fig. 1), being located almost symmetrically around the (119) and (229) peaks, which belong to the $Sr_9Ni_7O_{21}$ phase. Such characteristic pattern may indicate the presence of a new phase. Further studies are necessary, however in order to substantiate the possible existence of the new compound and to reveal its crystal structure and chemical composition.

In order to investigate the subsolidus phase equilibria in the Sr–Ni–O system, selected samples were studied ex situ by annealing and quenching method and in situ by HTXRD between 500 and 950 °C in air. Annealing at 500 °C did not cause any significant changes on the XRD patterns, but increasing amount of $SrCO_3$ indicated that some ternary phases were decomposed to a little extent. It is believed that the decomposition

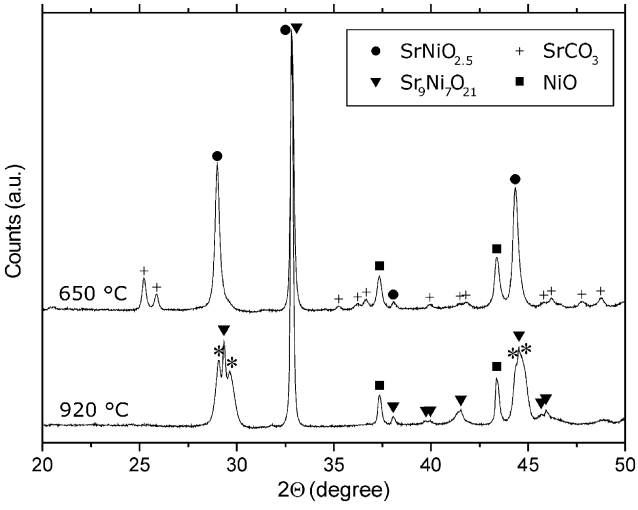

Fig. 1. XRD powder patterns of the SN3 sample (Sr:Ni atomic ratio = 49:51) prepared from nitrate solution, which was heat treated at two different temperatures and furnace cooled in air. Unidentified peaks are marked by stars.

products are NiO and SrO, the latter reacting immediately with atmospheric CO_2 thus forming carbonate phase. Around 700 °C, unidentified diffraction peaks in the SN3, SN5, and SN6 samples disappeared

completely, whereas $SrNiO_{2.5}$ and $Sr_5Ni_4O_{11}$ still existed metastably up to approximately 800 °C, due to the kinetic limitation. For instance, the fraction of $SrNiO_{2.5}$ diminished and the peaks of $SrCO_3$ and NiO became stronger upon increasing the annealing time at 700 °C from 1 to 8 h. Above 900 °C, only $Sr_9Ni_7O_{21}$, NiO and SrO were observed. Increasing annealing time from 1 to 8 h did not cause any changes on the HTXRD patterns. This three-phase mixture ($Sr_9Ni_7O_{21}$ + NiO + SrO) appears to be the equilibrium one and preserved, when the samples were cooled down to room temperature within 1 h.

Fig. 2 shows the TG (a) and DTA (b) curves obtained on heating the samples SN1, SN2, SN4, and SN5 in air up to 1295 °C with the rate of 5 °C min^{-1}. The investigated samples decomposed in two (SN1) or three steps (SN2, SN4, SN5). The corresponding plateaus on TG and endothermic effects on DTA curves are clearly seen in Fig. 2. In summary, thermal stability of ternary phases in the Sr–Ni–O system can be represented by the following reactions:

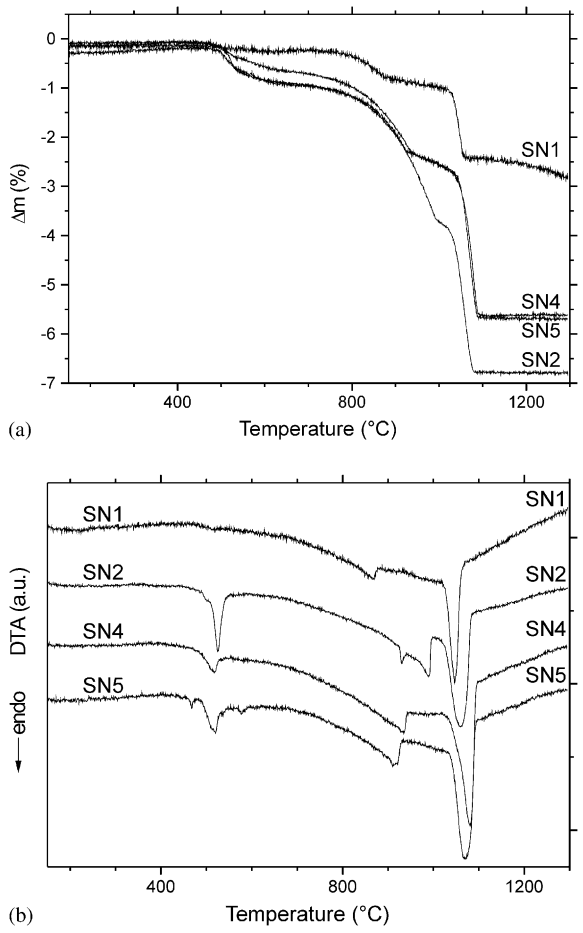

Fig. 2. TG (a) and DTA (b) results for selected samples prepared from nitrate solution. The samples were heat treated at 670 °C (SN2, SN4) or 920 °C (SN1, SN5) and furnace cooled in air. Heating in air with 5 °C min^{-1}.

$$SrNiO_{2.5} \rightarrow SrO + NiO + O_2,\ 480 \pm 5\,^{\circ}C \quad (1)$$

$$SrNiO_{2.5} \rightarrow Sr_9Ni_7O_{21} + NiO,\ \sim 800\,^{\circ}C \quad (2)$$

$$Sr_5Ni_4O_{11} \rightarrow Sr_9Ni_7O_{21} + NiO,\ \sim 800\,^{\circ}C \quad (3)$$

$$Sr_9Ni_7O_{21} \rightarrow SrO + NiO + O_2,\ 1030 \pm 6\,^{\circ}C \quad (4)$$

Such reaction scheme is consistent with XRD and TG/DTA results: the first thermal effect can be associated with the reaction (1), while the second plateau on the TG curve of the SN2, SN4 and SN5 samples is reached, when the reactions (2) and (3) are completed and the last decomposition step corresponds to the reaction (4). The final decomposition products in all cases were SrO and NiO as confirmed by XRD analysis. On cooling from 1295 °C to room temperature with 5 °C min^{-1} no thermal effects and no weight gain were observed. At the same time, ternary Sr–Ni–O phases listed in Table 3 are not metastable, since only endothermic effects were observed on DTA heating curves (Fig. 2b). It seems that heating to 1295 °C result in formation of coarse-grained SrO and NiO, which are unable to react at lower temperatures. All the ternary phases in the Sr–Ni–O system seem to possess some homogeneity range with respect to oxygen content, so that the observed weight loss (Fig. 2a) is a cumulative effect of decomposition and oxygen evolution. It is the oxygen non-stoichiometry of $Sr_9Ni_7O_{21}$ that is responsible for the minor weight loss in the SN1 sample below 874 °C.

4.3. The (Sr,Ni)O solid solution

For a quantitative determination of terminal solubilities in the SrO–NiO subsystem, the SN3 sample was heat-treated in air at 1350 °C for 96 h. Lattice parameters of SrO and NiO phases determined by XRD and the corresponding reference values are given in Table 4. A very small but measurable increase of lattice parameter of NiO was observed. In the case of SrO, measured lattice parameter was the same as for pure SrO within the limits of experimental errors. Since both the SrO and NiO crystallize in the same structure type, Vegard's law can be applied to estimate terminal solubilities. Simple calculation showed that NiO can

Table 4
Lattice parameters of SrO and NiO phases in the sample SN3 after heat treatment in air at 1350 °C for 96 h and terminal solubilities as determined from Vegard's law

Phase	Lattice parameter (nm)		Terminal solubility	
	This work	[17]	SrO (mol%)	NiO (mol%)
SrO	0.51600(4)	0.51600	100.00	0.00
NiO	0.41775(1)	0.41771	0.04(1)	99.96(1)

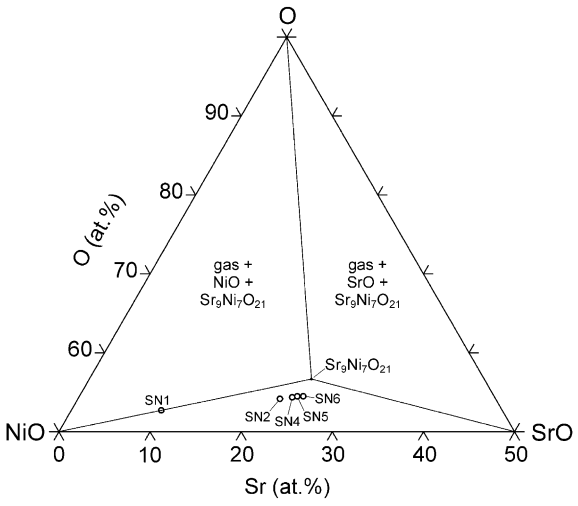

Fig. 3. Isothermal section of the SrO–NiO–O subsystem at 950–1030 °C. The oxygen partial pressure in the gas phase corresponds to the atmospheric air ($p_{O2} = 0.209$ atm). The investigated compositions (second series samples only) are shown as circles, where the oxygen content was calculated from the weight loss during the last decomposition step (Fig. 2a).

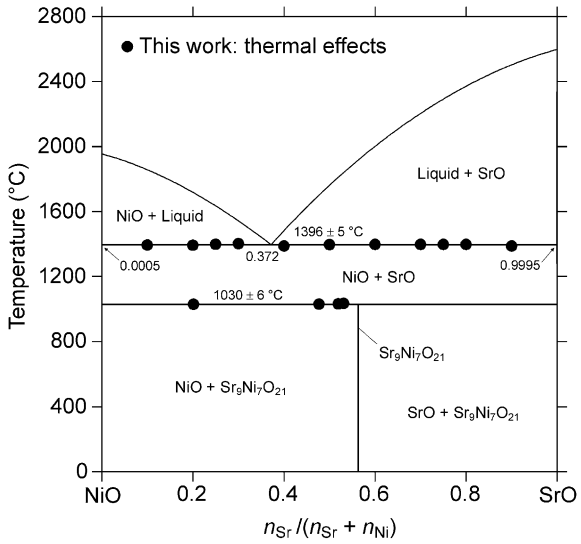

Fig. 4. Isobaric projection of phase equilibria in the Sr–Ni–O system on the NiO–SrO plane in air ($p_{O2} = 0.209$ atm). Lower part ($T < 1350$ °C)—experimental, upper part—calculated.

dissolve up to 0.04 mol% SrO, while the solubility of NiO in SrO is probably lower than 0.01 mol% (Table 4).

4.4. Phase diagram of the Sr–Ni–O system

Fig. 3 shows phase equilibria in the SrO–NiO–O subsystem at 950–1030 °C in air. Only one ternary compound, $Sr_9Ni_7O_{21}$ is stable at these conditions. The possible oxygen deficiency in this phase is small enough to be neglected. $Sr_9Ni_7O_{21}$ coexists with NiO, SrO and the gas phase. It can be seen that the composition of the SN1 sample is located exactly on the tie line NiO + $Sr_9Ni_7O_{21}$, while the samples SN2, SN4, SN5, and SN6 fall into the tie-triangle NiO + $Sr_9Ni_7O_{21}$ + SrO.

Fig. 4 shows an isobaric projection of phase equilibria in the Sr–Ni–O system onto SrO–NiO plane in air. The $SrNiO_{2.5}$ and $Sr_5Ni_4O_{11}$ phases are not shown here. It is believed that these two compounds are unstable in air, but form at higher oxygen activity, which was realized during decomposition of nitrate solutions. Indeed, after furnace cooling in air neither $SrNiO_{2.5}$ nor $Sr_5Ni_4O_{11}$ were observed. The phase diagram below 1350 °C is drawn according to the experimental results of this study. The upper part, e.g., the liquidus and solidus lines as well as the eutectic horizontal were calculated using a regular solution approximation. The Gibbs energy of the liquid and solid solutions is given by:

$$G^{liq} = x_{SrO}{}^{o}G^{liq}_{SrO} + x_{NiO}{}^{o}G^{liq}_{NiO} + RT(x_{SrO}\ln x_{SrO} + x_{NiO}\ln x_{NiO}) + x_{SrO}x_{NiO}{}^{0}L^{liq}_{SrO,NiO}, \quad (5)$$

$$G^{hal} = x_{SrO}{}^{o}G^{hal}_{SrO} + x_{NiO}{}^{o}G^{hal}_{NiO} + RT(x_{SrO}\ln x_{SrO} + x_{NiO}\ln x_{NiO}) + x_{SrO}x_{NiO}{}^{0}L^{hal}_{SrO,NiO}, \quad (6)$$

where superscripts liq and hal denote the liquid- and halite-type (Sr,Ni)O phases, respectively, x_{SrO}, x_{NiO} stand for the mole fractions of components, R is the gas constant, T is the absolute temperature (K), and ${}^{0}L$ are so-called *interaction parameters*, which account for the deviation from the ideal mixing behavior. The Gibbs energy functions for pure substances were taken from literature [19,20], while the interaction parameters were adjusted to fit the eutectic temperature and the terminal solubility of SrO in NiO at 1350 °C. The best match between calculated and experimental values is achieved with ${}^{0}L^{liq}_{SrO,NiO} = -52\,kJ\,mol^{-1}$ and ${}^{0}L^{hal}_{SrO,NiO} = +105\,kJ\,mol^{-1}$.

5. Conclusions

The constitution of the Sr–Ni–O system was studied experimentally for the first time. The mutual solubility of SrO and NiO is negligible (around 0.04 mol% at 1350 °C). The results of theoretical calculations, where the solubility was estimated to be around 25 mol% [11] are thus not supported by experimental evidence. In the SrO–NiO quasibinary system there is an eutectic reaction: liquid ⇔ SrO + NiO at 1396 °C and 37.2 mol% SrO in the liquid phase. Parameters of the regular solution model, which describes thermodynamic properties of liquid- and rocksalt-type (Sr,Ni)O solid

solution were estimated as -52 and $+105\,kJ\,mol^{-1}$, respectively.

Three ternary compounds were found to exist in the Sr–Ni–O system: $SrNiO_{2.5}$, $Sr_5Ni_4O_{11}$, and $Sr_9Ni_7O_{21}$, none of them can be prepared by a direct reaction between SrO (or $SrCO_3$) and NiO, but form, if the water solution of Sr- and Ni-nitrates is evaporated and thermally decomposed in air. It was demonstrated that $Sr_5Ni_4O_{11}$ and $Sr_9Ni_7O_{21}$ can be obtained not only from KOH melts, as reported in the literature, but also by the solid-state reaction. $Sr_9Ni_7O_{21}$ exists as stable phase in air up to 1030 °C, while $SrNiO_{2.5}$ and $Sr_5Ni_4O_{11}$ seem to require higher oxygen activity for their stabilization.

The isothermal section of the SrO–NiO–O subsystem at 950–1030 °C in air shows the presence of only one ternary compound, $Sr_9Ni_7O_{21}$, which form tie-lines with NiO, SrO and the gas phase.

Acknowledgments

The authors wish to express their thanks to Tanya Mayer, Albrecht Meyer, Horst Kummer, Gerhard Kaiser, Martina Thomas, Sandra Geupel, Nuri Solak, Ute Schäfer, and Hartmut Labitzke, Max-Planck-Institut für Metallforschung Stuttgart, for technical assistance and Prof. Dr. Fritz Aldinger for critical reading of the manuscript.

References

[1] M. Strunk, H. Müller-Buschbaum, J. Alloys Compd. 209 (1994) 189–192.
[2] M. Arjomand, D.J. Machin, J. Chem. Soc. Dalton Trans. 11 (1975) 1055–1061.
[3] F. Abraham, S. Minaud, C. Renard, J. Mater. Chem. 4 (1994) 1763–1764.
[4] M. Evain, F. Boucher, O. Gourdon, V. Petricek, M. Dusek, P. Bezdicka, Chem. Mater. 10 (1998) 3068–3076.
[5] J. Campa, E. Gutierrez-Puebla, A. Monge, I. Rasines, C. Ruiz-Valero, J. Solid State Chem. 108 (1994) 230–235.
[6] J. Campa, E. Gutierrez-Puebla, A. Monge, I. Rasines, C. Ruiz-Valero, J. Solid State Chem. 126 (1996) 27–32.
[7] R.D. Shannon, C.T. Prewitt, Acta Cryst. B 25 (1969) 925–946.
[8] H. von Wartenberg, E. Prophet, Z. Anorg. Allg. Chem. 208 (1932) 369–379.
[9] D.E. Smith, T.Y. Tien, L.H. Van Vlack, J. Am. Ceram. Soc. 52 (1969) 459–460.
[10] J.J. Lander, J. Am. Chem. Soc. 73 (1951) 2450–2452.
[11] B. Revzin, J. Pelleg, in: Thermodynamics and Kinetics of Phase Transformations, Materials Research Society Symposium Proceedings, Pittsburgh, vol. 398, 1996, pp. 649–654.
[12] H. Pausch, H. Müller-Buschbaum, Z. Anorg. Allg. Chem. 426 (1976) 184–188.
[13] Y. Takeda, T. Hashino, H. Miyamoto, F. Kanamaru, S. Kume, M. Koizumi, J. Inorg. Nucl. Chem. 34 (1972) 1599–1601.
[14] J.G. Lee, G.F. Holland, J. Solid State Chem. 93 (1991) 267–271.
[15] P.N. Bityutsky, V.I. Khitrova, Kristallografiya 29 (1984) 450–454.
[16] M.G. Harwood, N. Herzfeld, S.L. Martin, Trans. Farad. Soc. 46 (1950) 650–653.
[17] International Centre for Diffraction Data (ICDD), 12 Campus Boulevard, Newtown Square, PA, USA, http://www.icdd.com/, 2005.
[18] Inorganic Crystal Structure Database (ICSD), FIZ Karlsruhe, Germany, http://icsdweb.fiz-karlsruhe.de/, 2005.
[19] J.R. Taylor, A.T. Dinsdale, Z. Metallkd. 81 (1990) 354–366.
[20] D. Risold, B. Hallstedt, L.J. Gauckler, Calphad 20 (1996) 353–361.